Molecular Biology of the Cell
Vol. 18, 4762–4771, December 2007

Golgi-bound Rab34 Is a Novel Member of the Secretory Pathway[D]

Neil M. Goldenberg,* Sergio Grinstein,† and Mel Silverman‡

*Institute of Medical Science and ‡Department of Medicine, University of Toronto, Toronto, ON, Canada, M5S 1A8; and †Program in Cell Biology, Hospital for Sick Children, Toronto, ON, Canada, M5G 2C4

Submitted November 6, 2006; Revised September 5, 2007; Accepted September 11, 2007
Monitoring Editor: Jennifer Lippincott-Schwartz

Golgi-localized Rab34 has been implicated in repositioning lysosomes and activation of macropinocytosis. Using HeLa cells, we undertook a detailed investigation of Rab34 involvement in intracellular vesicle transport. Immunoelectron microscopy and immunocytochemistry confirmed that Rab34 is localized to the Golgi stack and that active Rab34 shifts lysosomes to the cell center. Contrary to a previous report, we found that Rab34 is not concentrated at membrane ruffles and is not involved in fluid-phase uptake. Also, Rab34-induced repositioning of lysosomes does not affect mannose 6-phosphate receptor trafficking. Most strikingly, HeLa cells depleted of Rab34 by transfection with dominant-negative Rab34 or after RNA interference, failed to transport the temperature-sensitive vesicular stomatitis virus G-protein (VSVG) fused to green fluorescent protein (VSVG-GFP) from the Golgi to the plasma membrane. Transfection with mouse Rab34 rescued this defect. Using endogenous major histocompatibility complex class I (MHCI) as a marker, an endoglycosidase H resistance assay showed that endoplasmic reticulum (ER) to medial Golgi traffic remains intact in knockdown cells, indicating that Rab34 specifically functions downstream of the ER. Further, brefeldin A treatment revealed that Rab34 effects intra-Golgi transport, not exit from the *trans*-Golgi network. Collectively, these results define Rab34 as a novel member of the secretory pathway acting at the Golgi.

INTRODUCTION

Rab GTPases and their effectors are involved in virtually all aspects of transport vesicle budding, movement, targeting, and fusion (Zerial and McBride, 2001). Different rab proteins have, in addition to a specific complement of effector proteins, a distinct compartmental distribution allowing them to perform numerous functions within cells (Grosshans *et al.*, 2006). The array of rab effectors—which includes enzymes, cytoskeletal elements, SNARE proteins, and vesicle coat proteins—combines with the tightly regulated intracellular distribution of rab proteins to allow rabs to perform a wide variety of cellular functions.

Constitutive secretion is governed by a defined set of Rab GTPases. Endoplasmic reticulum (ER)-to-Golgi transport requires Rab1 and Rab2 (Tisdale *et al.*, 1992; Allan *et al.*, 2000), Rab6 has been linked with intra-Golgi transport (Echard *et al.*, 2000), and transport from the *trans*-Golgi network (TGN) to the plasma membrane has been shown to involve Rab8 and Rab11 (Huber *et al.*, 1993; Chen *et al.*, 1998). This list, however, is not exhaustive, and whether other Rab proteins and their effectors are involved in constitutive secretion remains to be seen.

Little has been written about Golgi-bound rab, Rab34. Two effectors of Rab34 have been identified: the Rab-interacting lysosomal protein (RILP), which links Rab34 to dynein microtubule motors (Wang and Hong, 2002), and hmunc13, a protein kinase C superfamily member, which has been implicated in the induction of apoptosis at the Golgi in response to phorbol ester treatment (Speight and Silverman, 2005). By transfecting cell lines with constitutively active or dominant-negative forms of Rab34, Rab34 has been implicated in fluid-phase uptake of proteins at membrane ruffles via macropinocytosis (Sun *et al.*, 2003) and in the shifting of lysosomes toward the microtubule organizing center (MTOC; Wang and Hong, 2002).

To clarify the role of Rab34 in mammalian cells, we have used transiently transfected HeLa cells as a model system. Using green fluorescent protein (GFP) fusions of wild-type (wt-GFP-Rab34), constitutively active (CA-GFP-Rab34), or dominant-negative Rab34 (DN-GFP-Rab34), we have re-examined the existing literature pertaining to Rab34 and investigated new functional roles for Rab34 in HeLa cells. Because Rab34 is localized to the Golgi in our system, we sought to investigate Rab34 function in the context of this organelle. To this end, we used RNA interference (RNAi) to knock down Rab34 expression in HeLa cells. Using this assay, as well as the CA and DN Rab34 constructs used in the studies mentioned above, we re-evaluated the functions of Rab34 that have been described in the literature and examined the role of Rab34 in the secretory pathway. In our

This article was published online ahead of print in *MBC in Press* (http://www.molbiolcell.org/cgi/doi/10.1091/mbc.E06–11–0991) on September 19, 2007.

[D] The online version of this article contains supplemental material at *MBC Online* (http://www.molbiolcell.org).

Address correspondence to: Mel Silverman (melvin.silverman@utoronto.ca).

Abbreviations used: BFA, brefeldin A; CA-GFP-Rab34, GFP-tagged constitutively active Rab34; DN-GFP-Rab34, GFP-tagged dominant-negative Rab34; EndoH, endoglycosidase H; GFP, green fluorescent protein; HRas-Tail-RFP, RFP-tagged tail of H-Ras; MHC, major histocompatibility complex; M6PR, mannose 6-phosphate receptor; PI4P, phosphoinositol 4-phosphate; PKD, protein kinase D; RFP, red fluorescent protein; TGN, *trans*-Golgi network; TPA, 2-*O*-tetradecanoyl-phorbol 13-acetate; VSVG, vesicular stomatitis virus G protein; WGA, wheat germ agglutinin; wt-GFP-Rab34, GFP-tagged wild-type Rab34.

system, we are unable to observe any enrichment of Rab34 at membrane ruffles or any effect of Rab34 on fluid-phase uptake. Active Rab34, however, did cause lysosomes to shift to a juxtanuclear position, consistent with a previous report. The mechanism and functional implications of this phenotype are unclear, but we have determined that trafficking of the mannose 6-phosphate receptor (M6PR) is unaffected by Rab34. More strikingly, our data indicate that Rab34 is confined to the Golgi, where it is required for the exit of transport carriers traversing the secretory pathway. Our data show specifically that Rab34 is required for exit of vesicular stomatitis virus G-protein (VSVG)-GFP from the Golgi stack, upstream of the *trans*-Golgi network (TGN). This site of action places Rab34 upstream of several other known players in the secretory pathway, including protein kinase D (PKD) and phosphatidylinositol 4-phosphate (PI4P; Liljedahl *et al.*, 2001; Hausser *et al.*, 2005).

MATERIALS AND METHODS

Antibodies and Reagents

The following primary antibodies were used: rabbit anti-Rab34 (Santa Cruz Biotechnology, Santa Cruz, CA), mouse anti-GM130 (BD Biosciences, Palo Alto, CA), mouse anti-mannose 6-phosphate receptor (Calbiochem, La Jolla, CA), rabbit anti-GFP (Molecular Probes, Eugene, OR), mouse anti-LAMP-1 (Developmental Studies Hybridoma Bank, University of Iowa, Iowa City, IA), mouse anti-Vinculin (Sigma, St. Louis, MO), and mouse anti-MHC class I W6/32 (a gift from Dr. D. B. Williams, University of Toronto, Canada). Anti-mouse-Cy3 (Jackson ImmunoResearch, West Grove, PA) was used as a secondary antibody for immunofluorescence, and anti-rabbit-HRP and anti-mouse-HRP (Santa Cruz) were used for Western blotting. Rhodamine-conjugated wheat germ agglutinin (WGA) was from Vector Laboratories (Burlingame, CA), Alexa-647–conjugated WGA was from Molecular Probes. Alexa-647–conjugated dextran was from Molecular Probes. Protein A-Sepharose (GE Healthcare, Waukesha, WI) was used for immunoprecipitation, and [^{35}S]methionine was from Amersham Biosciences (Piscataway, NJ). Nocodazole, 2-O-tetradecanoyl-phorbol 13-acetate (TPA), and brefeldin A (BFA) were from Sigma. The ceramide analog D-threo-1-phenyl-2-decanoylamino-3-morpholino-1-propanol (PDMP) was from BIOMOL (Plymouth Meeting, PA).

Plasmids and Small Interfering RNA

Wild-type Rab34 fused to the C-terminal of GFP (wt-GFP-Rab34) was constructed using Gateway Technology (Invitrogen, Carlsbad, CA) with pcDNA-DEST40-Rab34wt (described in Speight and Silverman, 2005) as donor, and pcDNA6.2/N-EmGFP-DEST as the destination vector. Both the CA GTP-restricted, Q111L mutant and the DN GDP-restricted, T66N mutants were fused to GFP using the same method (CA-GFP-Rab34 and DN-GFP-Rab34, respectively). The pEGFPdKA206K-N1-VSVG tsO45 vector encoding VSVG-GFP and pEGFPdKA206K-N1-mCherry (VSVG-Cherry) were generous gifts from Dr. J. Lippincott-Schwartz (NIH, Bethesda, MD). Plasmids encoding the tail of H-Ras fused to red fluorescent protein (RFP; HRas-tail-RFP), the PH domain of phospholipase c-delta (PLCδ -PH-RFP), or GPI-linked RFP (GPI-RFP) have been described previously (Varnai and Balla, 1998; Choy *et al.*, 1999; Keller, 2001). Stealth small interfering RNA (siRNA) directed against human Rab34 and appropriate scrambled control siRNA were synthesized by Invitrogen. siRNA targeting Rab34 was the following annealed duplex: 5′AAUCGUUCCAUCUCGAAGUCCACUC3′ and 5′GAGUGGACUUCGAGAUGGAACGAUU3′.

Cell Culture and Transfection

HeLa cells were grown in MEM plus 10% fetal bovine serum and maintained at 37°C in 5% CO_2. Transfection of siRNA was performed using Lipofectamine 2000 (Invitrogen) according to the manufacturer's directions. Plasmid DNA was transfected using FuGene 6 Reagent (Roche, Indianapolis, IN) according to the manufacturer's directions, using a DNA:FuGene ratio of 3:1.

Cryo-Electron Microscopy

HeLa cells were grown in 10-cm dishes and transfected with GFP-Rab34-wt. Twenty-four hours after transfection, cells were washed in phosphate-buffered saline (PBS) and fixed in 4% followed by 8% paraformaldehyde. Cells were then washed in 0.15 M glycine, followed by 1% gelatin in PBS. Cells were scraped, pelleted, and resuspended in 12% gelatin. The cells were then pelleted again and cooled to allow the gelatin to set. The pellets were cut into 1-mm^3 pieces and put in 2.3 M sucrose in PBS at 4°C overnight. The sucrose pieces were put on metal pins, frozen in liquid nitrogen, and sectioned at −120°C at a thickness of 75 nm. Sections were picked up in a 1:1 mixture of 2% methyl cellulose and 2.3 M sucrose and transferred to formvar-coated nickel grids. For immunostaining, sections were blocked in 5% fish skin gelatin and then incubated for 30 min in anti-GFP. Sections were washed and incubated with protein A-Gold, then washed, and fixed in 1% glutaraldehyde. Phosphate was removed in water, and the sections were stained in methylcellulose and uranyl acetate on ice.

Immunoblotting

Cells were lysed in 1% NP-40, and protein concentration in lysates was determined using a Lowry assay (Bio-Rad, Richmond, CA). Fifty micrograms of protein was run on a 10% polyacrylamide gel. After transfer to nitrocellulose, filters were blocked in 5% nonfat dry milk powder in 10 mM Tris-HCl (pH 8.0), 150 mM NaCl, and 0.05% Tween 20 (TBST) overnight at 4°C. Primary and secondary antibodies were diluted in blocking buffer, and incubations were for 1 h at room temperature. Detection was performed using an ECL Advance Western Blotting Detection Kit (Amersham Biosciences).

Membrane Ruffling and Dextran Uptake

HeLa cells were cotransfected with wt-GFP-Rab34 and either HRas-tail-RFP or PLCδ-PH-RFP. After 24 h, membrane ruffling was induced by treatment with 100 nM TPA for 10 min in HEPES-buffered MEM, and the cells were imaged live using a spinning disk confocal microscope (Leica, Deerfield, IL), and the fluorescence intensity of GFP both at a ruffle and nonruffle, as well as for RFP at a ruffle and nonruffle was measured using ImageJ (NIH). The ratio of ruffle to nonruffle fluorescence for GFP was divided by the ratio of ruffle to nonruffle fluorescence for RFP to determine whether or not Rab34 was specifically enriched at membrane ruffles.

To measure dextran uptake, HeLa cells transfected with GFP-Rab34 vectors or with GFP alone were exposed to 200 μg/ml Alexa-647 Dextran for 10 min. Cells were then rinsed in ice-cold PBS, trypsinized, and analyzed by fluorescence-activated cell sorting (FACS). Transfected cells (n = 10,000) were counted for each experimental condition. Data were analyzed using FlowJo (Tree Star, Ashland, OR), and Alexa-647-dextran fluorescence was expressed as a percent of Alexa-647 fluorescence in cells transfected with GFP alone.

Lysosomal Positioning Assay

HeLa cells were transfected with Rab34 vectors and imaged 24 h after transfection. Cells were serum starved for 2 h and then were fixed in 3.7% paraformaldehyde, permeabilized in 0.2% Triton X-100, and blocked in 10% fat-free milk. Fixed cells were stained using anti-LAMP-1 antibody and Cy3-conjugated secondary antibody. Cells were visualized by confocal microscopy. Analysis was performed using the Radial Plot function in ImageJ (NIH). Rab34–expressing cells were identified by GFP fluorescence; using Radial Plot, concentric circles were drawn from the cell center to the cell boundary, and integrated LAMP-1 fluorescence intensities were recorded for the area along each circle. To normalize for cell size and fluorescence, the data were binned into the inner, middle, and outer thirds of each cell and expressed as a percent of total LAMP-1 fluorescence.

DN and CA Rab34 Assays

HeLa cells plated on glass coverslips in 12-well plates were transfected with one of wt-GFP-Rab34, CA-GFP-Rab34, or DN-GFP-Rab34. For M6PR experiments, cells were fixed in 3.7% paraformaldehyde 24 h after transfection, permeabilized, and stained with anti-M6PR and anti-mouse Cy3. Cells were mounted and imaged using a spinning disk confocal microscope (Leica). For VSVG-Cherry experiments, cells were cotransfected with GFP-Rab34 or its mutants, as well as VSVG-Cherry at 40°C as described below.

VSVG-GFP Secretion Assay

HeLa cells were plated on glass coverslips in 12-well plates. The following day, cells were transfected with either scrambled small interfering RNA (siRNA) or siRNA directed against Rab34 and incubated for 48 h. After this, cells were transfected with VSVG-GFP and incubated at 40°C for a further 20 h. All subsequent incubations were done in the presence of 50 μg/ml cycloheximide (Sigma) to halt protein synthesis. For time t = 0, cells were rinsed in ice-cold PBS before fixation. Remaining cells were returned to an incubator at 32°C for the indicated time. After incubation, cells were rinsed in ice-cold PBS and fixed in 3.7% paraformaldehyde. For treatment with WGA, cells were incubated with 0.01 mg/ml WGA on ice for 10 min. For GM130 staining, cells were permeabilized with 0.2% Triton X-100 and stained using anti-GM130, followed by a Cy3-anti-mouse antibody. Cells were mounted on slides and imaged using a Zeiss LSM 510 confocal microscope (Thornwood, NY). Image analysis was performed using Volocity (Improvision, Lexington, MA).

Endoglycosidase H Assay

HeLa cells were plated in 60-mm dishes, transfected with either scrambled siRNA or siRNA against Rab34, and incubated for 72 h. Metabolic labeling, immunoprecipitation and endoglycosidase H (EndoH) digestion were performed as described (Kim *et al.*, 1996). Briefly, cells were incubated for 30 min in RPMI lacking methionine. Metabolic labeling was performed using 150 μCi of [^{35}S]methionine per plate for 10 min. Chase incubations were done in RPMI

supplemented with methionine for the indicated times. After chase, cells were rinsed in ice-cold PBS and lysed in buffer containing NP40. For immunoprecipitation of major histocompatibility complex (MHC) class I molecules, each lysate was incubated in anti-MHC class I antibody W6/32, followed by protein A-Sepharose. After washing, lysates were split, and some were incubated with endoH (New England Biolabs, Beverly, MA) for 3 h at 37°C. Samples were then run on 10% polyacrylamide gels.

RESULTS

GFP-Rab34 Is Localized to the Golgi

Wt-GFP-Rab34 was expressed in HeLa cells, and several protocols were initiated to evaluate the differing claims in the literature regarding Rab34 localization. When cells are fixed and immunostained with the Golgi marker, GM130, wt-GFP-Rab34 and GM130 colocalize at the Golgi (Figure 1). Moreover, the near-complete colocalization of wt-GFP-Rab34 and GM130 persists after microtubule depolymerization with nocodazole (Figure 1). To determine the precise localization of Rab34 in the Golgi stack, we used immunogold labeling of transfected wt-GFP-Rab34 in ultrathin cryosections of fixed HeLa cells. Transmission electron microscopy revealed that wt-GFP-Rab34 is present throughout the Golgi stack, both in the Golgi cisternae and on a population of Golgi-associated vesicles (Figure 1B). Transfected wt-GFP-Rab34 is seen on some *cis*-Golgi transport carriers, as well as on some peri-Golgi transport vesicles (arrowheads in Figure 1B). The vast majority of labeling is observed in the Golgi cisternae themselves, and there is no preference for *cis*-, medial-, or *trans*-Golgi stacks. Similarly, wt-GFP-Rab34 is relatively evenly distributed within each cisterna, with no preference for central or terminal membranes.

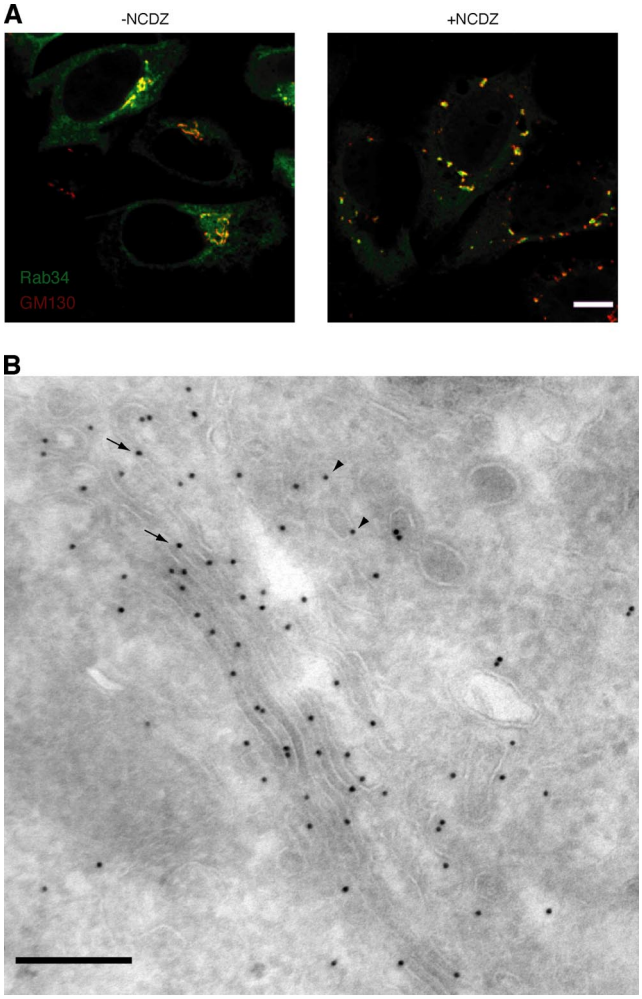

Figure 1. Rab34 is localized to the Golgi in HeLa cells. (A) HeLa cells transiently transfected with wt-GFP-Rab34 were treated with or without nocodazole (ncdz) to depolymerize microtubules, and were fixed and stained for the Golgi marker, GM130. Note the colocalization of wt-GFP-Rab34 and GM130 both in the absence (−ncdz) and presence (+ncdz) of nocodazole, suggesting Golgi localization. Scale bar, 10 μm. (B) HeLa cells transiently transfected with wt-GFP-Rab34 were fixed and processed for immunoelectron microscopy as described in *Materials and Methods*. Immunogold labeling shows wt-GFP-Rab34 is present throughout the Golgi stack (arrows), as well as on some *cis*-Golgi and peri-Golgi vesicular elements (arrowheads). Scale bar, 200 nm.

Rab34 Is Not Concentrated at Membrane Ruffles

It has been reported previously that Rab34 is recruited to sites of membrane ruffling, where it is involved in macropinocytosis (Sun *et al.*, 2003). Membrane ruffles are accumulations of lipid, protein, and cytoskeletal elements at the plasma membrane in response to several stimuli, including

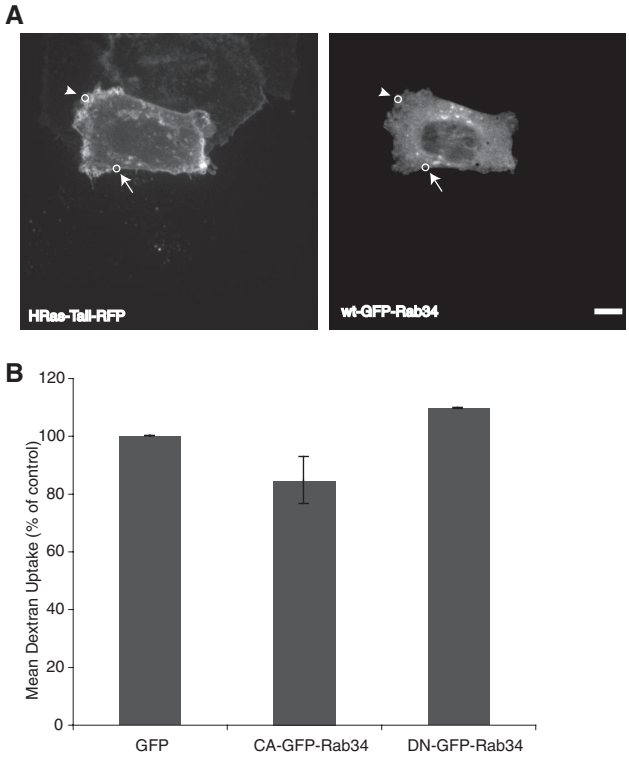

Figure 2. Golgi-bound Rab34 is not concentrated at membrane ruffles and does not participate in fluid-phase uptake. (A) HeLa cells coexpressing wt-GFP-Rab34 and HRas-Tail-RFP were treated with 100 nM TPA for 10 min, and the live cells were imaged using a spinning disk confocal microscope. Fluorescence intensities were measured for each channel at either membrane ruffles (arrowheads) or a nonruffled area of plasma membrane (arrows). Scale bar, 12 μm. (B) FACS analysis of dextran uptake. HeLa cells expressing CA-GFP-Rab34, DN-GFP-Rab34, or GFP alone were serum-starved and allowed to take up Alexa-647–labeled dextran for 10 min. Cells were harvested, and dextran uptake in Rab34-transfected cells was analyzed for 10,000 transfected (GFP-positive) cells per transfection condition. Dextran uptake was expressed as mean Alexa-647 fluorescence, normalized to Alexa-647 fluorescence for cells transfected with GFP alone ($p > 0.1$, $n = 3$). Data are shown ±SE.

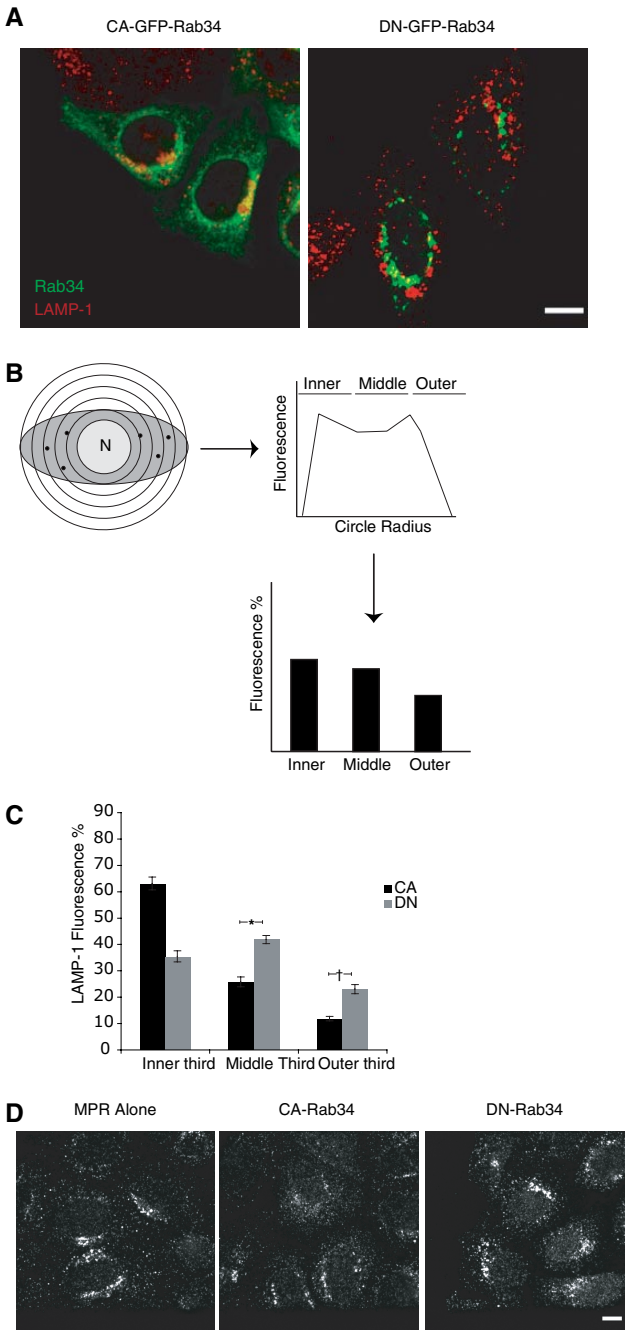

Figure 3. Active Rab34 shifts lysosomes toward the MTOC, but does not effect the M6PR. (A) HeLa cells transfected with either CA-GFP-Rab34 or DN-GFP-Rab34 were fixed and stained with a mAb against LAMP-1 to mark lysosomes. Cells were imaged by confocal microscopy. Scale bar, 10 μm. (B) To quantitate the position of lysosomes relative to the cell center, the Radial Plot plugin was used, as described in *Materials and Methods*. This plugin records the integrated lysosomal fluorescence (black dots) along circles of increasing radius from the nucleus (N). To normalize for variable cell size and fluorescence intensities, these data were binned into one of the inner, middle, or outer thirds of the cell, and expressed as a percent of total LAMP-1 fluorescence. (C) Quantitated data from the method described in B. CA, CA-GFP-Rab34; DN ; DN-GFP-Rab34. n = 20 cells were analyzed per condition; $^{*}p < 0.01$, $^{\dagger}p < 0.05$. Results are shown ±SE. Scale bar, 10 μm. (D) HeLa cells were fixed directly, or transiently transfected with either CA-GFP-Rab34 (CA-Rab34) or DN-GFP-Rab34 (DN-Rab34), serum-starved, fixed, and stained for M6PR. Cells were imaged using a spinning disk confocal microscope. The GFP signal was used to locate transfected cells, but is not shown for the purpose of clarity. All cells in these representative fields were transfected with the indicated GFP-Rab34 constructs. HeLa cells transfected with either CA- or DN-GFP-Rab34 showed no significant changes from controls, suggesting that Rab34 does not effect M6PR trafficking. Scale bar, 12 μm.

phorbol esters and growth factors (Kurokawa and Matsuda, 2005). Because membrane ruffles are such high density structures and because membrane ruffles change the 3D structure of cells, it can be difficult to ascertain by confocal microscopy whether a protein is truly recruited to a membrane ruffle or if this is an artifact that arises from an accumulation of cell density at the ruffled region.

In an effort to examine a potential role for Rab34 in membrane ruffling in HeLa cells, we coexpressed wt-GFP-Rab34 with the tail of H-Ras fused to RFP (HRas-Tail-RFP). HRas-Tail-RFP inserts into the plasma membrane by three palmitate moieties and is therefore a consistent marker for the plasma membrane (Roy *et al.*, 2005). These cells were then treated with 100 nm TPA for 10 min to induce membrane ruffling, and live cells were subsequently analyzed by spinning disk confocal microscopy (Figure 2). For each of the GFP and RFP channels, a ratio of fluorescence intensity was taken at a membrane ruffle (Figure 2, arrowheads) and compared with an area of the plasma membrane that has not undergone ruffling (Figure 2, arrows). The Rab34 ratio was then divided by the HRas-Tail ratio to correct for membrane density changes at the membrane ruffle. If Rab34 is truly recruited to membrane ruffles, this ratio should be greater than 1. In our HeLa cell system, we found that Rab34 is not recruited to membrane ruffles, because the ratio of Rab34 signals to HRas-Tail signals was 0.98, which was not significantly different from 1 ($p > 0.5$, $n = 20$). To further demonstrate the lack of Rab34 recruitment to membrane ruffles, this experiment was repeated with another membrane marker. This time, the pleckstrin-homology domain of phospholipase c-delta fused to RFP (PLCδ-PH-RFP), which binds phosphoinositides in the plasma membrane (Stauffer *et al.*, 1998), was coexpressed with wt-Rab34-GFP, and the same assay and quantification was performed as described above. Similar to what was observed with HRas-Tail, the ratio of Rab34 to PLCδ-PH-RFP was not found to differ significantly from 1, strongly supporting the observation that Rab34 is not concentrated at sites of membrane ruffling in HeLa cells (ratio = 1.10, $p > 0.3$, $n = 20$; data not shown).

Rab34 Does Not Participate in Fluid-Phase Uptake

It has also been previously reported that active Rab34 increases macropinocytosis, even in the absence of stimuli such as phorbol esters or platlet-derived growth factor (Sun *et al.*, 2003). To test whether Rab34 affects fluid-phase uptake in our HeLa cell system, we transfected HeLa cells with CA-GFP-Rab34, DN-GFP-Rab34, or GFP alone. Cells were then incubated for 10 min with Alexa-647–conjugated dextran as a tracer for fluid-phase uptake. To perform a quantitative, high-throughput analysis of dextran uptake, we used FACS to determine the amount of dextran taken up by our transfected cells (Figure 2B). For each transfection condition, 10,000 transfected cells were analyzed. Contrary to the previous report, but consistent with our finding that Rab34 is not recruited to membrane ruffles in HeLa cells, we found that Rab34 did not effect dextran uptake in HeLa cells, because neither CA-GFP-Rab34 nor DN-GFP-Rab34 cells exhibited a significant change in dextran uptake when compared with

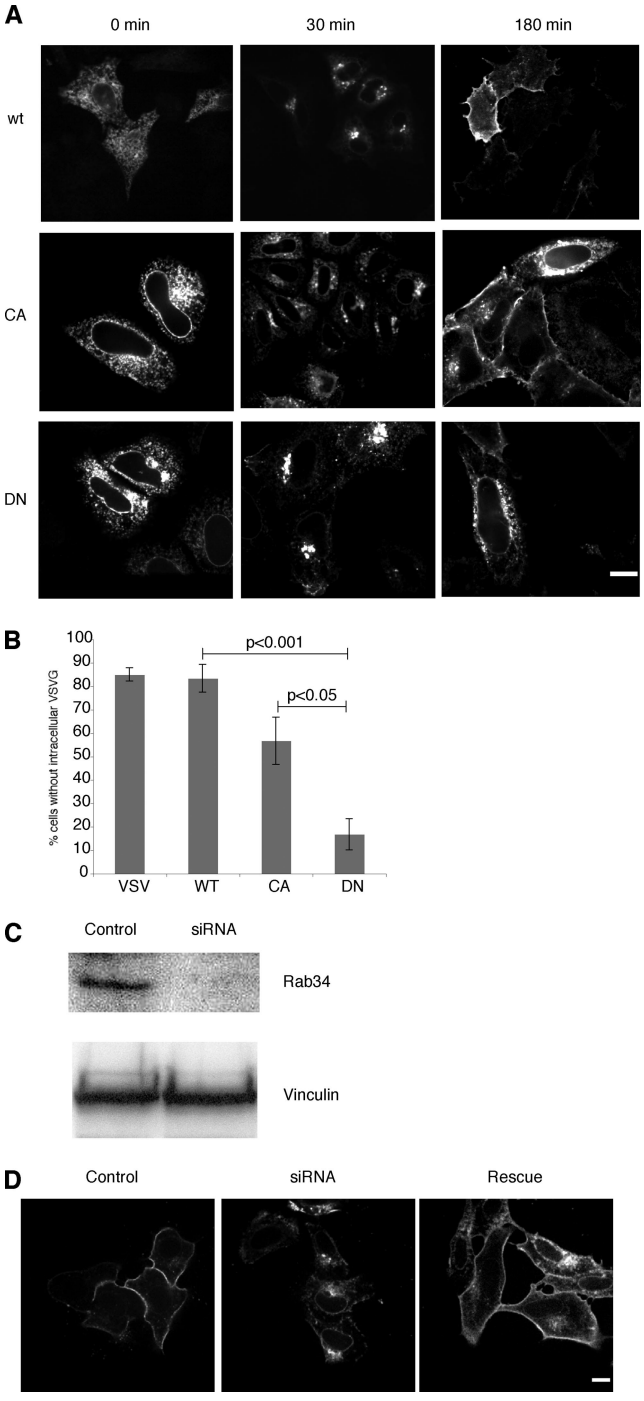

Figure 4. Dominant-negative Rab34 or siRNA inhibit VSVG-Cherry transport from the Golgi to the plasma membrane. (A) HeLa cells were cotransfected with VSVG-Cherry and one of wt-, CA-, or DN-GFP-Rab3, and incubated overnight at 40°C. Cells were treated with cycloheximide and were shifted to 32°C at t = 0 min to allow VSVG transport to occur. Cells were fixed at the indicated times and imaged using a spinning disk confocal microscope. Scale bar, 12 μm. (B) Quantification of the results in A. Cells treated as in A were scored at t = 180 min for the proportion of cells showing complete transport of VSVG-Cherry to the plasma membrane. At least 20 cells were counted per condition for each of three independent experiments. The conditions examined were VSVG-Cherry alone (VSV), or VSVG-Cherry plus one of wt-GFP-Rab34 (WT), CA-GFP-Rab34 (CA), or DN-GFP-Rab34 (DN). Note the marked inhibition of Golgi to plasma membrane transport in cells expressing DN-GFP-Rab34 ($p < 0.001$ compared with wild type). (C) Knockdown of endogenous Rab34 in HeLa cells. HeLa cells were transfected with siRNA directed against human Rab34 or scrambled control siRNA. After 72 h, cells were lysed and analyzed by Western blot with a polyclonal anti-Rab34 antibody. Shown is a representative gel from three experiments. As a loading control, membranes were probed for vinculin. (D) HeLa cells transfected with scrambled siRNA (control) or siRNA against Rab34 (siRNA) were transfected with VSVG-Cherry 48 h later and incubated overnight at 40°C. Cells were shifted to the permissive temperature and fixed after 180 min. Note that Rab34 siRNA arrests VSVG-Cherry transport at the Golgi. In the third panel, cells transfected with Rab34 siRNA were then cotransfected with VSVG-Cherry and GFP-mRab34. Note that GFP-mRab34 is capable of rescuing the defect seen in siRNA cells, demonstrating the specificity of the Rab34 siRNA treatment. Scale bar, 12 μm.

HeLa cells transfected with GFP alone. Mean dextran fluorescence values of 111 and 103% of uptake in cells expressing GFP alone were found for CA-GFP-Rab34 and DN-GFP-Rab34, respectively, and were not statistically significant ($p > 0.05$, n = 3). It is possible that the finding observed by Sun *et al.* (2003) represents a cell-specific phenomenon.

Rab34 Regulates Lysosomal Position, But Does Not Affect the Localization of the Mannose 6-Phosphate Receptor

The other phenotype previously associated with active Rab34 was its ability to shift lysosomes toward the MTOC via its association with RILP and the dynein/dynactin system (Wang and Hong, 2002). To test this phenomenon in our HeLa cell system, HeLa cells were transfected with either CA-GFP-Rab34 or DN-GFP-Rab34, fixed, and stained with an anti-LAMP-1 antibody to visualize lysosomes. To quantitate lysosomal position relative to the nucleus, we used a system of concentric circles drawn from the cell center, as described in *Materials and Methods* (Figure 3). Lysosomal position was then calculated as the percent of LAMP-1 fluorescence in a given cell within either the inner, middle, or outer third of the cell itself. We found that CA-GFP-Rab34 caused a significant shift of LAMP-1 fluorescence to the inner third of the cell as compared with DN-GFP-Rab34: 63% of the LAMP-1 fluorescence was found in the inner third of cells transfected with CA-GFP-Rab34 versus 35% for DN-GFP-Rab34 ($p < 0.01$). This finding suggests that the work of Wang and Hong (2002) in Normal Rat Kidney cells can be generalized into our HeLa cell system.

Because active Rab34 was able to reposition lysosomes in HeLa cells, we next asked whether this positional change might be indicative of a change in TGN-to-lysosome trafficking. To examine this possibility, we used an antibody to the cation-independent M6PR. The M6PR is responsible for the trafficking of acid hydrolases from the TGN to the endosome (Ghosh *et al.*, 2003). Once in the endosome, the M6PR and its ligand travel to the lysosomal compartment, where acidic pH results in the dissociation of ligand from the receptor, at which time the M6PR recycles back to the TGN (Ghosh *et al.*, 2003). HeLa cells that had been transfected with either CA-GFP-Rab34 or DN-GFP-Rab34 were fixed and immunostained with an M6PR antibody (Figure 3D). In untransfected cells, the M6PR resides in both a juxtanuclear compartment as well as a punctate, endosomal compartment. This localization did not significantly change in HeLa cells expressing either Rab34 mutant, suggesting that Rab34 does not have a role in TGN to lysosome trafficking (Figure 3D). Therefore, the repositioning of lysosomes by active Rab34 is unlikely to be involved in the transport of acid hydrolases to the late endosome/lysosome.

Rab34 Is Required for Secretion of VSVG-GFP at the Golgi

Because Rab34 is localized to the Golgi, we wanted to test whether Rab34 may be involved in the secretory pathway. As a reporter for constitutive secretion, we used the ts045 temperature-sensitive mutant of the VSV glycoprotein fused to one of GFP (VSVG-GFP), or monomeric Cherry (VSVG-Cherry). The temperature-sensitive mutant is retained in the ER at 40°C, and is released into the secretory pathway upon temperature shift to 32°C. To study the potential role of Rab34 in the secretory pathway, HeLa cells were either transfected with VSVG-Cherry alone, or cotransfected with VSVG-Cherry, and one of wt-GFP-Rab34, CA-GFP-Rab34, or DN-GFP-Rab34 at 40°C. The following day, protein synthesis was inhibited with cycloheximide, and at t = 0 the cells were shifted to the permissive temperature of 32°C for various times. In cells expressing VSVG-Cherry alone or in combination with wt-GFP-Rab34, the VSVG protein was found in the ER at t = 0, predominantly at the Golgi at t = 30 min, with a small amount of protein still in the ER, and entirely at the plasma membrane at t = 180 min (Figure 4). Only a very small number of cells coexpressing VSV-Cherry and wt-GFP-Rab34 exhibited a delay of VSVG-Cherry transport to the plasma membrane. In contrast, HeLa cells expressing DN-GFP-Rab34 exhibited a marked decrease in VSVG-Cherry transport from the Golgi to the plasma membrane (Figure 4). Only 16.7% of cells expressing DN-GFP-Rab34 had transported all VSVG-Cherry to the plasma membrane, compared with 83% of cells expressing wt-GFP-Rab34, or 85% of cells expressing VSVG-Cherry alone ($p < 0.001$; Figure 4B). These results strongly suggest that Rab34 is required for secretion of VSVG-Cherry from the Golgi. Cells expressing CA-GFP-Rab34 also exhibited limited inhibition of VSVG-Cherry secretion to the plasma membrane, with 56.7% of cells completely transporting VSVG to the cell surface (Figure 4B). The effect of CA-GFP-Rab34 on VSVG-Cherry secretion suggests that there is a requirement for Rab34 to maintain the ability to cycle between the GTP- and GDP-bound states for normal trafficking of VSVG-Cherry to the plasma membrane. This phenomenon has been observed for other small GTPases as well, including Rac and Arf6 (Arrieumerlou *et al.*, 2000; Klein *et al.*, 2006).

To further study the role of Rab34 in the secretory pathway, we used RNAi by transfecting HeLa cells with siRNA to deplete cells of endogenous Rab34. Seventy-two hours after transfection, significant knockdown of endogenous Rab34 was observed in HeLa cells transfected with siRNA targeting Rab34, compared with cells transfected with scrambled siRNA (Figure 4C). HeLa cells that had been transfected with either siRNA targeting Rab34 or a scrambled control siRNA were then transfected with VSVG-GFP, incubated at 40°C for 20 h, and then treated with cycloheximide. After 180 min at the permissive temperature of 32°C, control HeLa cells transfected with scrambled siRNA had completely transported VSVG-Cherry to the plasma membrane (Figure 4D). Strikingly, HeLa cells transfected with siRNA directed against Rab34 exhibited an arrest of VSVG-Cherry transport. The vast majority of VSVG-Cherry remained in the Golgi, although there was a minor leak to the cell surface (Figure 4D). To further establish the specificity of our siRNA treatments, we sought to rescue the defect seen in siRNA-transfected cells. To this end, we used a GFP-fusion of wild-type mouse Rab34 (GFP-mRab34). The mouse Rab34 cDNA sequence differs from that of human Rab34 over the region of our siRNA, so this construct should be resistant to silencing by our siRNA transfection. HeLa cells that had been treated with siRNA to deplete endogenous Rab34 were cotransfected with VSVG-Cherry and GFP-mRab34 after 48 h. Using our standard protocol, these cells showed a marked rescue of VSVG-Cherry transport to the cell surface compared with cells that were not transfected with mRab34 (Figure 4D). Although not all cells showed a complete rescue, it was clear that the majority of VSVG-Cherry transport to the cell surface had been restored by GFP-mRab34. Taken together, these results define Rab34 as a novel member of the secretory pathway, acting at the Golgi.

To further define the precise site of action of Rab34, we performed a time course experiment along with quantitative colocalization of VSVG-GFP and either the Golgi or the plasma membrane. To this end, HeLa cells transfected with control siRNA or siRNA against Rab34 were transfected with VSVG-GFP and followed at the permissive temperature for either 0, 30, or 180 min. At each time point, cells were fixed and either immunostained for the Golgi with an anti-GM130 antibody or stained for the plasma membrane with rhodamine-conjugated WGA. Immediately after a temperature shift to 32°C, all VSVG-GFP was found in the ER in both control and knockdown cells, and after 30 min, the majority of VSVG-GFP had traveled to the Golgi (Figure 5A, i–iv and vii–x). In control cells, at 180 min after temperature shift, virtually all VSVG-GFP was found at the plasma membrane (Figure 5Av). In contrast, in cells depleted of Rab34, very little VSVG-GFP was found at the plasma membrane, and the majority of the protein was retained in the Golgi (Figure 5A, compare v and vi). At 180 min after temperature shift, Pearson's coefficients for VSVG-GFP and WGA for control cells and knockdown cells of 0.82 and 0.44, respectively, show that although the majority of VSVG-GFP in control cells colocalized with the plasma membrane, much less of the GFP signal colocalized with WGA in cells depleted of endogenous Rab34 ($p < 0.001$; Figure 5B). Furthermore, although in control cells very little GFP signal was seen colocalizing with GM130 at the Golgi (Pearson's coefficient of 0.16), a significant amount of GFP signal remains in the Golgi in cells depleted of Rab34 3 h after release from the ER (Pearson's coefficient of 0.47, $p < 0.001$; Figure 5, C and B, compare xi and xii). The large increase in Pearson's coefficients from 0 to 30 min after temperature shift shows that VSVG-GFP is efficiently transported to the Golgi in both control and knockdown cells (for example, Pearson's coefficient for GFP and GM130 increases from 0.23 to 0.73, and from 0.29 to 0.78 in control and knockdown cells, respectively). Because Pearson's coefficients for 0 and 30 min time points do not differ significantly between control cells and those lacking Rab34, it appears that ER-to-Golgi transport is not affected by Rab34 knockdown, suggesting that Rab34 functions at a post-Golgi step in the secretory pathway. The small proportion of VSVG-GFP that is still transported to the plasma membrane in knockdown cells is probably due to either incomplete knockdown of Rab34 in these cells or to the existence of both Rab34-dependent and -independent pathways from the Golgi to the plasma membrane.

Rab34 Depletion Arrests Intra-Golgi Transport of VSVG-GFP, Not Golgi-to-TGN Transport

Several molecules have been implicated in VSVG-GFP release from the TGN, including PKD and PI4P (Liljedahl *et al.*, 2001; Hausser, 2005). Using conventional light microscopy and colocalization techniques, it is difficult to determine whether a protein is found in the *trans*-Golgi cisternae or in the TGN, which lies distal to the *trans*-

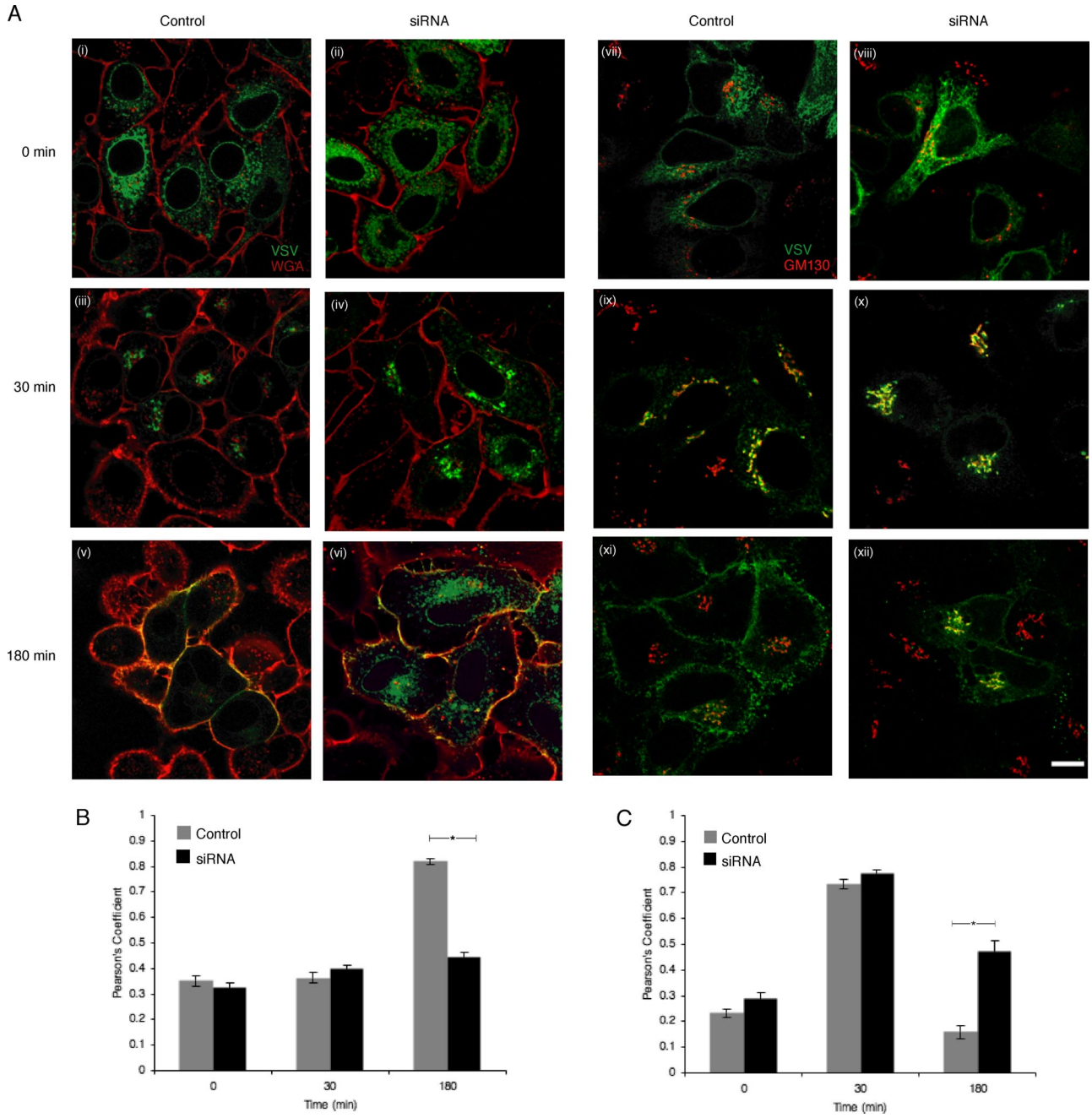

Figure 5. Rab34 is necessary for exit of VSVG-GFP from the Golgi. (A) VSVG-GFP secretion assay. HeLa cells were transfected with siRNA directed against Rab34 (siRNA) or scrambled control siRNA (control). Forty-eight hours later, cells were transfected with plasmid encoding VSVG-GFP and incubated at 40°C for 20 h. After cycloheximide treatment, the temperature was shifted to 32°C, and cells were fixed at the indicated time points and stained with a monoclonal anti-GM130 antibody to mark the Golgi or with WGA to mark the plasma membrane. Scale bar, 10 μm. Images are representative of greater than three experiments. (B) Colocalization of VSVG-GFP and WGA. Pearson's coefficients were calculated for 18 cells per condition from at least three experiments. Data are shown $\pm$SE. *$p < 0.001$. (C) As in B, but for colocalization of VSVG-GFP and GM130.

Golgi itself in the secretory pathway. To explore the precise location of the effect of Rab34 on VSVG-GFP secretion, we exploited the toxin BFA. BFA treatment is known to result in the retrograde transport of Golgi-resident proteins into the ER (Lippincott-Schwartz *et al.*, 1990). The TGN, on the other hand, in response to BFA treatment, condenses in the juxtanuclear region (Chege and Pfeffer, 1990). This differential effect of BFA on *trans*-Golgi versus TGN-resident proteins allows for careful dissection of these two compartments. To this end, we performed our VSVG-GFP secretion assay in HeLa cells transfected with siRNA directed against Rab34 or the appropriate controls. At either t = 30 or 180 min, cells were treated with 5 μg/ml BFA for 30 min before fixation and imaging by spinning disk confocal microscopy (Figure 6). At t = 30 min, both control cells (30 min ctrl) and knockdown cells (30 min siRNA) show VSVG-GFP to be in the Golgi stack. BFA treatment confirms this, resulting in redistribution of

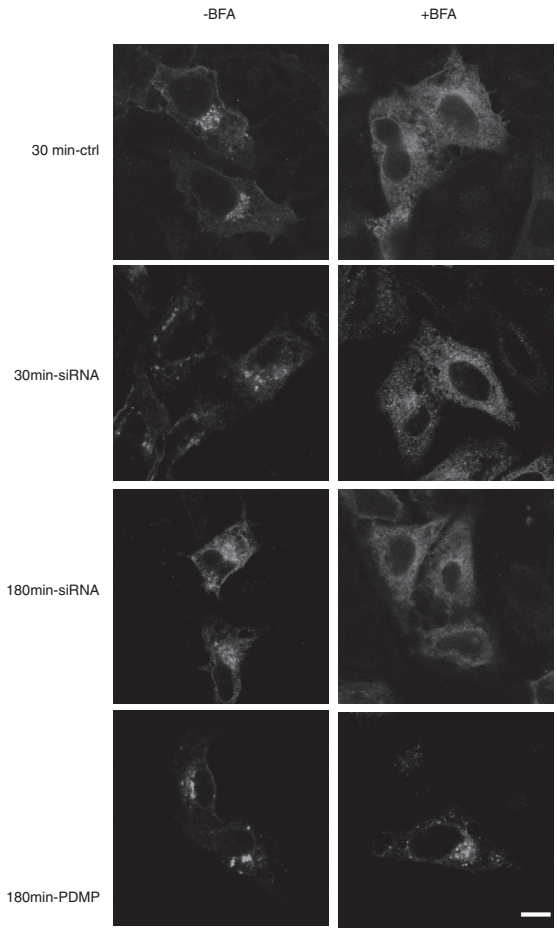

Figure 6. Rab34 is required for intra-Golgi transport of VSVG-GFP, not exit from the TGN. HeLa cells transfected with siRNA directed against Rab34 or scrambled control were transfected with VSVG-GFP at 40°C. At t = 0, cells were treated with cycloheximide and shifted to the permissive temperature of 32°C. At t = 30 or 180 min, cells were treated for 30 min with BFA at 32°C, fixed, and viewed using a spinning disk confocal microscope. At t = 30 min, cells transfected with control siRNA (30 min-ctrl) or Rab34 siRNA (30 min-siRNA) had VSVG-GFP in the Golgi. After 30-min BFA treatment (+BFA), GFP signal redistributed to the ER. At t = 180 min, Rab34 siRNA-treated cells (180 min-siRNA) retained VSVG-GFP in the Golgi, and BFA treatment (+BFA) redistributed the GFP signal to the ER. As a control, cells treated with PDMP retained VSVG-GFP in the TGN at t = 180 min (180 min-PDMP), as BFA treatment (+BFA) resulted in the condensation of the GFP signal in the juxtanuclear region. Scale bar, 10 μm.

VSVG-GFP to the ER (Figure 6, top four panels). At t = 180 min, knockdown cells (180 min-siRNA) show that VSVG-GFP remains in the Golgi, and BFA treatment again results in the redistribution of the GFP signal to the ER (Figure 6). These data suggest that Rab34 is required for intra-Golgi transport of VSVG-GFP, not Golgi to TGN transport. As a control, cells were treated with the ceramide analog, PDMP. PDMP has been shown to block VSVG-GFP transport at the TGN as a result of defective protein ADP-ribosylation (De Matteisa *et al.*, 1999). At t = 180 min, PDMP-treated cells also contain VSVG-GFP in the Golgi, but BFA treatment fails to redistribute the GFP signal to the ER (Figure 6, bottom panels). The VSVG-GFP protein condenses into a discrete pocket in the juxtanuclear region, suggesting a TGN localization of VSVG-GFP in PDMP-treated HeLa cells, demonstrating the differential effect of BFA on Golgi and TGN-resident proteins.

Collectively, the above experiments show that Rab34 is required for intra-Golgi transport of VSVG-GFP in HeLa cells. This result places Rab34 upstream of PKD and PI4P in the secretory pathway.

Rab34 Is Not Involved in ER-to-Golgi Transport

Although confocal microscopy suggested that Rab34 was not involved in the transport of proteins from the ER to the Golgi, we sought to examine this step of the secretory pathway biochemically using endogenous MHC class I protein as a reporter. HeLa cells transfected with either scrambled siRNA or siRNA targeting Rab34 were metabolically labeled with a pulse of [^{35}S]methionine, and then chased with cold methionine for 0–60 min. Total MHC class I was immunoprecipitated from cell lysates and subsequently digested with endoH. EndoH cleaves N-linked oligosaccharides on proteins in the ER, but cannot cleave the high-mannose oligosaccharides found on proteins that have progressed to the medial Golgi (Orlean *et al.*, 1991). Thus, proteins in the ER are endoH sensitive, and proteins that have progressed to the Golgi are endoH resistant. This difference can be seen as a mobility shift on a polyacrylamide gel. As seen by the rates of acquisition of endoH resistance by endogenous MHC class I protein, depletion of endogenous Rab34 has no effect on ER-to-Golgi transport in HeLa cells (Supplementary Figure S1). Taken with the VSVG-GFP secretion data, these results show that Rab34 specifically functions at a post-Golgi step of the secretory pathway. Further, because EndoH resistance is acquired in the medial Golgi, Rab34 must function at a transport step at or beyond the medial Golgi.

DISCUSSION

Previous reports have proposed various roles and subcellular localizations for Rab34 (Wang and Hong, 2002; Sun *et al.*, 2003; Speight and Silverman, 2005). In the face of several published phenotypes, we sought to clarify the role of Rab34 first by reevaluating the literature in our HeLa cell system and then by depleting HeLa cells of endogenous Rab34 using RNAi. Our findings limit Rab34 localization to the Golgi and cast doubt upon its suggested role at the plasma membrane. The use of both fluorescence microscopy and immunoelectron microscopy have shown that wild-type GFP-Rab34 is localized to the Golgi stack, as well as to a population of *cis*-Golgi elements and intra-Golgi transport carriers. The report by Sun *et al.* (2003) led us to examine the potential role of Rab34 at membrane ruffles in HeLa cells. Our attempts to establish this role using quantitative colocalization with plasma membrane markers in HeLa cells were not successful. Clearly further work must be done before one can safely conclude that Rab34 is recruited to membrane ruffles in a manner that can be generalized to multiple cell types. We also found that Rab34 has no effect on fluid-phase uptake in HeLa cells. These results suggest that the findings of Sun *et al.* (2003) may represent a cell-specific phenomenon.

From the Golgi, our data demonstrate two roles for Rab34, which need not be completely independent of one another. First, we found that active Rab34 is capable of shifting lysosomes to the juxtanuclear region, which is consistent with published literature (Wang and Hong, 2002). Our finding with the greatest functional significance, however, is that Rab34 is required for the intra-Golgi transport of the model

protein cargo, VSVG-GFP, as it traverses the secretory pathway. Using three separate methods—namely siRNA, dominant-negative Rab34, and rescue of the siRNA-mediated defect—we have shown that Rab34 is a novel member of the secretory pathway. HeLa cells depleted of Rab34 by RNAi or dominant-negative Rab34 expression exhibited a marked decrease in transport of VSVG-GFP from the Golgi to the plasma membrane. The defect seen in siRNA-transfected cells can be rescued by expression of mouse Rab34, indicating that this phenomenon is specifically due to Rab34 depletion. This result establishes Rab34 as an essential player in a ubiquitous cellular function.

Both fluorescence microscopy of VSVG-GFP transport and rates of acquisition of endoH resistance of endogenous MHC showed that secretory transport from the ER to the medial Golgi remains intact in the absence of Rab34, because the medial Golgi is the site of high mannose glycosylation of transmembrane proteins (Orlean *et al.*, 1991). This result, in combination with those described above, shows that Rab34 acts either within or immediately after the Golgi stack.

Because Rab34 is involved in intra-Golgi protein transport, one would expect that an effect would be seen on both the trafficking of VSVG and the trafficking of the M6PR, because this transport step is upstream of TGN sorting. Because no clear effect was seen on the steady-state distribution of the M6PR, two possibilities exist. One is that the effect on the M6PR is subtler than the effect on VSVG. Our data in Figure 4D may provide clues that although a gross change in M6PR distribution is not occurring, a smaller-scale change in M6PR trafficking may be present in HeLa cells transfected with Rab34 mutants. Further work involving dynamic measurements of M6PR trafficking to the endosomal system in the presence of Rab34 mutants and compartmental markers is required in order to elucidate a potential function for Rab34 in this pathway. A second possibility is that Rab34 exhibits cargo selectivity within the Golgi. Although this may be an intriguing possibility, much more work needs to be done to attempt to define a mechanism by which this could occur.

Although our data support the finding that Rab34 is capable of moving lysosomes toward the MTOC, the functional implications of lysosomal position remain unknown. From the Golgi, at least two pathways for vesicle traffic depart—the classic secretory pathway to the plasma membrane, for which we have shown Rab34 to be necessary, and another pathway to the late endosome/lysosome. This second pathway is necessary for the delivery of acid hydrolases to the maturing lysosome (Ghosh *et al.*, 2003). Because Rab34 appears to be involved in the transport of proteins through the Golgi along the secretory pathway, it is tempting to hypothesize that it is also involved in trafficking to the lysosome and that increased Golgi-to-lysosome traffic by active Rab34 may be occurring while lysosomes shift toward the Golgi. However, as discussed above, dominant-negative and CA Rab34 did not grossly affect the localization of the M6PR in HeLa cells, although a more subtle effect could not be ruled out. Thus, the significance of the phenotype characterized by Rab34 induced movement of lysosomes toward the MTOC remains to be determined.

Although the mechanism by which Rab34 affects lysosomal position has been shown to require interaction with RILP, which links Rab34 to the dynein/dynactin microtubule motor system (Wang and Hong, 2002), the mechanism by which Rab34 effects secretion from the Golgi is less clear. To date, only two effectors have been identified for Rab34—RILP, and hmunc13, which is a well-described PKC superfamily member that is involved in both vesicle priming and the induction of apoptosis at the Golgi in response to phorbol ester treatment (Augustin *et al.*, 1999; Song *et al.*, 1999). To determine the mechanism of Rab34 function in constitutive secretion, we first sought to define the precise site of action of Rab34 in the secretory pathway. BFA treatment revealed that Rab34 depletion arrests VSVG-GFP transport within the Golgi itself, not at the TGN. This result mechanistically separates the function of Rab34 from that of known mediators of TGN exit.

The exit of proteins from the TGN has been reported to involve PKD, as well as Golgi-resident sphingolipids and PI4P (Rosenwald *et al.*, 1992; Echard *et al.*, 2000; Liljedahl *et al.*, 2001; Hausser, 2005). Dominant-negative PKD inhibits the fission of transport carriers from the TGN, and its expression results in extensive tubulation of the TGN, indicative of a release failure of these extending tubules from the TGN (Liljedahl *et al.*, 2001). Although it is known that Golgi-resident diacylglycerol is responsible for the recruitment of PKD to the Golgi, the molecular mechanism of PKD-mediated transport carrier fission has not been completely defined (Baron and Malhotra, 2002). It is known, however, that PKD can activate phosphatidylinositol 4-kinase III-β, resulting in an increase in TGN PI4P, which is in turn required for vesicle fission (Hausser , 2005). It has also been shown that inhibition of de novo sphingolipid synthesis inhibits VSVG transport along the secretory pathway (Rosenwald *et al.*, 1992). The importance of sphingolipids in this process is not known, but the Golgi is a key store of ceramide and sphingolipids (Rosenwald *et al.*, 1992). Our work establishes that Rab34 functions upstream of these components of the secretory pathway.

Rab6A is involved in transport of VSVG through the Golgi itself (Echard *et al.*, 2000). Interestingly, it is CA Rab6A, not DN Rab6A, that inhibits secretion through the Golgi. This sets up an intriguing possibility whereby Rab6A and Rab34 may act in opposition to one another, because active Rab6A or loss of Rab34 inhibit secretion. It is possible that these two inputs could allow the cell to control constitutive secretion at the Golgi in response to various stimuli. Future experiments will seek to define the precise molecular events of Rab34-mediated transport, as well as defining cellular regulators of Rab34 activity.

Finally, it is interesting to examine our results in the light of the findings by Wang and Hong (2002) showing that Rab34 regulates lysosomal positioning from the Golgi. Their data describe a pathway whereby Rab7-positive lysosomes migrate along microtubules to the peri-Golgi region via an association between Rab7, RILP, and Golgi-bound Rab34 (Wang and Hong, 2002). This region appears to be particularly active, housing the Golgi, TGN, recycling endosomes, lysosomes, and various other components of the endomembrane system. In addition, at this same location within the cell, our lab has previously shown that hmunc13 interacts with GTP-bound Rab34 via its second munc homology domain (Speight and Silverman, 2005). Although it is premature to indulge in significant speculation at this point, it seems possible that a situation exists whereby regulated formation of a molecular platform occurs involving protein interactions between Rab34, Rab7, RILP, hmunc13, and probably as yet other unidentified proteins.

ACKNOWLEDGMENTS

We greatly appreciate the work of Bob Temkin at The Advanced Bioimaging Centre at The University of Toronto. This work was funded by Canadian Institutes of Health Research (CIHR) Grant FRN-15071 to M.S. N.M.G. is supported by a CIHR MD/PhD Studentship.

REFERENCES

Allan, B. B., Moyer, B. D., and Balch, W. E. (2000). Rab1 recruitment of p115 into a cis-SNARE complex: programming budding COPII vesicles for fusion. Science *289*, 444–448.

Arrieumerlou, C., Randriamampita, C., Bismuth, G., and Trautmann, A. (2000). Rac is involved in early TCR signaling. J. Immunol. *165*, 3182–3189.

Augustin, I., Rosenmund, C., Sudhof, T. C., and Brose, N. (1999). Munc13-1 is essential for fusion competence of glutamatergic synaptic vesicles. Nature *400*, 457–461.

Baron, C. L., and Malhotra, V. (2002). Role of diacylglycerol in PKD recruitment to the TGN and protein transport to the plasma membrane. Science *295*, 325–328.

Chege, N. W., and Pfeffer, S. R. (1990). Compartmentation of the Golgi complex: brefeldin-A distinguishes trans-Golgi cisternae from the trans-Golgi network. J. Cell Biol. *111*, 893–899.

Chen, W., Feng, Y., Chen, D., and Wandinger-Ness, A. (1998). Rab11 is required for trans-Golgi network-to-plasma membrane transport and a preferential target for GDP dissociation inhibitor. Mol. Biol. Cell *9*, 3241–3257.

Choy, E., Chiu, V. K., Silletti, J., Feoktistov, M., Morimoto, T., Michaelson, D., Ivanov, I. E., and Philips, M. R. (1999). Endomembrane trafficking of ras: the CAAX motif targets proteins to the ER and Golgi. Cell *98*, 69–80.

De Matteisa, M. A., Lunab, A., Di Tullioa, G., Cordaa, D., Kokc, J. W., Luinia, A., and Egeab, G. (1999). PDMP blocks the BFA-induced ADP-ribosylation of BARS-50 in isolated Golgi membranes. FEBS Lett. *459*, 310–312.

Echard, A., Opdam, F.J.M., de Leeuw, H.J.P.C., Jollivet, F., Savelkoul, P., Hendriks, W., Voorberg, J., Goud, B., and Fransen, J.A.M. (2000). Alternative splicing of the human Rab6A gene generates two close but functionally different isoforms. Mol. Biol. Cell *11*, 3819–3833.

Ghosh, P., Dahms, N. M., and Kornfeld, S. (2003). Mannose 6-phosphate receptors: new twists in the tale. Nat. Rev. Mol. Cell Biol. *4*, 202–212.

Grosshans, B. L., Ortiz, D., and Novick, P. (2006). Rabs and their effectors: achieving specificity in membrane traffic. Proc. Natl. Acad. Sci. USA *103*, 11821–11827.

Hausser, A., S. P., Martens, S., Link, G., Toker, A., Pfizenmaier, K. (2005). Protein kinase D regulates vesicular transport by phosphorylating and activating phosphatidylinositol-4 kinase IIIbeta at the Golgi complex. Nat. Cell Biol. *7*, 851–853.

Huber, L. A., Pimplikar, S., Parton, R. G., Virta, H., Zerial, M., and Simons, K. (1993). Rab8, a small GTPase involved in vesicular traffic between the TGN and the basolateral plasma membrane. J. Cell Biol. *123*, 35–45.

Keller, P., T. D., Diaz, E., White, J., Simons, K. (2001). Multicolour imaging of post-Golgi sorting and trafficking in live cells. Nat. Cell Biol. *3*, 140–149.

Kim, J. H., Lingwood, C. A., Williams, D. B., Furuya, W., Manolson, M. F., and Grinstein, S. (1996). Dynamic measurement of the pH of the Golgi complex in living cells using retrograde transport of the verotoxin receptor. J. Cell Biol. *134*, 1387–1399.

Klein, S., Franco, M., Chardin, P., and Luton, F. (2006). Role of the Arf6 GDP/GTP cycle and Arf6 GTPase-activating proteins in actin remodeling and intracellular transport. J. Biol. Chem. *281*, 12352–12361.

Kurokawa, K., and Matsuda, M. (2005). Localized RhoA activation as a requirement for the induction of membrane ruffling. Mol. Biol. Cell *16*, 4294–4303.

Liljedahl, M., Maeda, Y., Colanzi, A., Ayala, I., Van Lint, J., and Malhotra, V. (2001). Protein kinase D regulates the fission of cell surface destined transport carriers from the trans-Golgi network. Cell *104*, 409–420.

Lippincott-Schwartz, J., Donaldson, J. G., Schweizer, A., Berger, E. G., Hauri, H. P., Yuan, L. C., and Klausner, R. D. (1990). Microtubule-dependent retrograde transport of proteins into the ER in the presence of brefeldin A suggests an ER recycling pathway. Cell *60*, 821–836.

Orlean, P., Kuranda, M. J., and Albright, C. F. (1991). Analysis of glycoproteins from *Saccharomyces cerevisiae*. Methods Enzymol. *194*, 682–697.

Rosenwald, A. G., Machamer, C. E., and Pagano, R. E. (1992). Effects of a sphingolipid synthesis inhibitor on membrane transport through the secretory pathway. Biochemistry *31*, 3581–3590.

Roy, S., Plowman, S., Rotblat, B., Prior, I. A., Muncke, C., Grainger, S., Parton, R. G., Henis, Y. I., Kloog, Y., and Hancock, J. F. (2005). Individual palmitoyl residues serve distinct roles in H-ras trafficking, microlocalization, and signaling. Mol. Cell. Biol. *25*, 6722–6733.

Song, Y., Ailenberg, M., and Silverman, M. (1999). Human munc13 is a diacylglycerol receptor that induces apoptosis and may contribute to renal cell injury in hyperglycemia. Mol. Biol. Cell *10*, 1609–1619.

Speight, P., and Silverman, M. (2005). Diacylglycerol-activated Hmunc13 serves as an effector of the GTPase Rab34. Traffic *6*, 858–865.

Stauffer, T. P., Ahn, S., and Meyer, T. (1998). Receptor-induced transient reduction in plasma membrane PtdIns(4,5)P2 concentration monitored in living cells. Curr. Biol. *8*, 343–346.

Sun, P., Yamamoto, H., Suetsugu, S., Miki, H., Takenawa, T., and Endo, T. (2003). Small GTPase Rah/Rab34 is associated with membrane ruffles and macropinosomes and promotes macropinosome formation. J. Biol. Chem. *278*, 4063–4071.

Tisdale, E. J., Bourne, J. R., Khosravi-Far, R., Der, C. J., and Balch, W. E. (1992). GTP-binding mutants of rab1 and rab2 are potent inhibitors of vesicular transport from the endoplasmic reticulum to the Golgi complex. J. Cell Biol. *119*, 749–761.

Varnai, P., and Balla, T. (1998). Visualization of phosphoinositides that bind pleckstrin homology domains: calcium- and agonist-induced dynamic changes and relationship to myo-[^{3}H]inositol-labeled phosphoinositide pools. J. Cell Biol. *143*, 501–510.

Wang, T., and Hong, W. (2002). Interorganellar regulation of lysosome positioning by the Golgi apparatus through Rab34 interaction with Rab-interacting lysosomal protein. Mol. Biol. Cell *13*, 4317–4332.

Zerial, M., and McBride, H. (2001). Rab proteins as membrane organizers. Nat. Rev. Mol. Cell Biol. *2*, 107–117.